A Stability Analysis of Finite-Volume Advection Schemes Permitting Long Time Steps

PETER HJORT LAURITZEN

National Center for Atmospheric Research, Boulder, Colorado*

(Manuscript received 30 May 2006, in final form 27 October 2006)

ABSTRACT

Finite-volume schemes developed in the meteorological community that permit long time steps are considered. These include Eulerian flux-form schemes as well as fully two-dimensional and cascade cell-integrated semi-Lagrangian (CISL) schemes. A one- and two-dimensional Von Neumann stability analysis of these finite-volume advection schemes is given. Contrary to previous analysis, no simplifications in terms of reducing the formal order of the schemes, which makes the analysis mathematically less complex, have been applied. An interscheme comparison of both dissipation and dispersion properties is given. The main finding is that the dissipation and dispersion properties of Eulerian flux-form schemes are sensitive to the choice of inner and outer operators applied in the scheme that can lead to increased numerical damping for large Courant numbers. This spurious dependence on the integer value of the Courant number disappears if the inner and outer operators are identical, in which case, under the assumptions used in the stability analysis, the Eulerian flux-form scheme becomes identical to the cascade scheme. To explain these properties a conceptual interpretation of the flux-based Eulerian schemes is provided. Of the two CISL schemes, the cascade scheme has superior stability properties.

1. Introduction

Finite-volume methods for numerical solutions to conservation laws, in particular the continuity equation stating the conservation of mass, have received increased attention in the meteorological literature during the last two decades. For a recent review of finite-volume methods in meteorology, see, for instance, Machenhauer et al. (2007). In fact, finite-volume schemes for the continuity equation of atmospheric constituents have become standard in transport modules in atmospheric models since they do not have spurious numerical sources or sinks of mass. This intrinsic conservation property is due to the discretized schemes being based on the equations of motion in differential form integrated over control volumes. Hence, finite-volume schemes are also referred to as cell-integrated schemes. To avoid the inconsistencies resulting from using wind and pressure data from dynamical cores using a numerical method for the mass continuity equation that is different from the one applied to the continuity equations for atmospheric constituents in the transport module (Jöckel et al. 2001), dynamical cores that also solve the continuity equation for air as a whole with cell-integrated methods have recently been developed (e.g., Lin 2004; Lauritzen et al. 2006b,c, manuscripts submitted to *Quart. J. Roy. Meteor. Soc.*).

Cell-integrated advection schemes can be divided into two categories: first, Eulerian-type schemes in which the flux of mass through regular (Eulerian) cell walls is tracked (e.g., Bott 1989; Hólm 1995; Lin and Rood 1996; Leonard et al. 1996), and second, semi-Lagrangian-type schemes in which the mass in cells moving with the flow is tracked (e.g., Rančić 1992; Laprise and Plante 1995; Machenhauer and Olk 1998; Nair and Machenhauer 2002; Nair et al. 2002; Zerroukat et al. 2002). To compute the fluxes through the cell walls in Eulerian schemes or the integral over deformed cells transported with the flow in semi-Lagrangian methods, some type of subgrid-scale reconstruction is needed. By far the most widely used method is the piecewise parabolic method (PPM) introduced by Colella and Woodward (1984). Despite the popularity of PPM, the dis-

* The National Center for Atmospheric Research is sponsored by the National Science Foundation.

Corresponding author address: Peter Hjort Lauritzen, Climate Modeling Section, Climate and Global Dynamics Division, National Center for Atmospheric Research, 1850 Table Mesa Drive, Boulder, CO 80305.
E-mail: pel@ucar.edu

DOI: 10.1175/MWR3425.1

persion and dissipation properties of schemes based on this method have (as far as the author is aware) only been assessed indirectly through idealized advection tests and not analytically in terms of a Von Neumann stability analysis. Lin and Rood (1996, hereafter referred to as LR96) have performed a simplified stability analysis in terms of a low order version of their scheme (see the appendix for comments on the LR96 stability analysis) and Zerroukat et al. (2006) have performed a detailed analytical error and convergence analysis of PPM. This article provides some theoretical insight into the stability properties of both lower- and higher-order versions of both one- and two-dimensional cell-integrated schemes used in meteorology.

Here we consider schemes formulated for the sphere that permit long time steps, that is, the Eulerian flux-form scheme of LR96 and the cell-integrated semi-Lagrangian (CISL) schemes of Nair and Machenhauer (2002, hereafter referred to as NM02) and Nair et al. (2002, hereafter referred to as NSS02). Also, the CISL scheme of Zerroukat et al. (2002) belongs to the above category, but under the assumptions made in the stability analysis, it becomes identical to the scheme of NSS02, of course, if the same one-dimensional operators are applied. Hence the Von Neumann stability analysis of the NSS02 scheme also applies to the scheme of Zerroukat et al. (2002). Note first that the LR96 scheme is often referred to as semi-Lagrangian in the literature since it permits long time steps although it is based on a Eulerian flux-form discretization, and second that the Conservative Operator Splitting for Multidimensions with Inherent Constancy (COSMIC) scheme in Leonard et al. (1996) and the LR96 scheme are practically identical.

The paper is organized as follows. In one dimension there is little ambiguity in the derivation of finite-volume schemes, and hence the stability analysis for the one-dimensional versions of the LR96, NM02, and NSS02 schemes becomes identical (section 2). The one-dimensional analysis is extended to two dimensions in sections 3a–c. Section 3d provides brief comments on the general application of these advection schemes such as the effect of limiters/filters and errors generated in complex flows. A summary of the Von Neumann stability analysis is given in section 4.

2. One-dimensional cell-integrated schemes

Consider the one-dimensional cell-integrated continuity equations for air as a whole and an atmospheric constituent:

$$\frac{d}{dt}\int_{\delta x}\psi(x)\,dx = 0, \tag{1}$$

where $\psi = \rho$ and $\psi = \rho Q$, respectively. Here ρ is the density of air, Q is the mixing ratio for the constituent in question, and δx is a length interval moving with the flow. For notational convenience, define the operator I:

$$I_A^x[\psi(x)] \equiv \frac{1}{A}\int_A \psi(x)\,dx = \overline{\psi}, \tag{2}$$

where A is the length interval over which $\psi(x)$ is integrated and the superscript x refers to the coordinate direction in which the integral is taken, and $\overline{\psi}$ is the average value of $\psi(x)$ over A. The upstream CISL as well as the Eulerian flux-form discretization of (1) can be written as

$$\overline{\psi}^{n+1}\Delta x = I^x_{\delta x^n_*}[\psi^n(x)]\delta x^n_* \tag{3}$$

(e.g., Laprise and Plante 1995), where n is the time-level index, Δx is the regular grid interval, $\overline{\psi}^{n+1}$ is the average of $\psi^{n+1}(x)$ over Δx, and δx^n_* the length interval whose boundaries end up at the boundaries of Δx after being transported by the wind over one time step. In the discretization $\psi^n(x)$ is not known and must be constructed from the known grid cell averages $\overline{\psi}^n$. This process is referred to as subgrid cell reconstruction. To have mass conservation the subgrid cell reconstruction must satisfy

$$I^x_{\Delta x}[\psi^n(x)] = \overline{\psi}^n, \tag{4}$$

and the cell walls of any particular departure cell must also be the left and right cell walls of the two neighboring cells, respectively. Contrary to cell-integrated schemes, an advective-form discretization is based on gridpoint values rather than cell averages. Hence the velocity components can be interpreted as unique to a particular control volume rather than individual cell faces (Leonard et al. 1996). Hence each cell moves as a solid body, and as a result neighboring cells in divergent flows may overlap and/or have cracks between them, causing a violation of mass conservation.

a. Subgrid cell reconstruction

Piecewise constant (Godunov 1959) and piecewise linear (van Leer 1977) subgrid cell reconstructions do, in general, lead to excessively diffusive schemes that make them unsuitable for atmospheric modeling. In general, to reduce the numerical damping to an acceptable level, higher-order polynomial reconstruction must be applied. On the other hand the computational cost of the subgrid cell reconstruction increases with the complexity of the reconstruction method, which partly

explains why parabolas are the predominant choice for subgrid-scale reconstructions. The most widespread method is the PPM, but alternatives exist such as the parabolic reconstruction method used in Laprise and Plante (1995), the piecewise cubic method defined by Zerroukat et al. (2002), the parabolic spline method (Zerroukat et al. 2006), and fifth- and higher- (odd) order methods used by Leonard et al. (1996). Note that although low-order schemes require less computational work per grid cell, it takes a large increase in resolution to obtain a given accuracy compared to higher-order unlimited schemes (e.g., Leonard et al. 1996). Up to a certain order (which varies with scheme), the gain in accuracy with higher-order methods that do not apply limiters/filters more than offsets the larger cost per grid cell update compared to low-order schemes. However, if the monotonic limiter of Colella and Woodward (1984) is employed, for example, the gain in accuracy for higher-order schemes mentioned above may be reduced or even eliminated because of the increased numerical diffusion induced by the filter (see also section 3d). In this analysis subgrid cell reconstructions based on the first-order piecewise constant method (PCM), second-order piecewise linear method (PLM), and third-order PPM are considered.

For simplicity assume an equidistant grid with grid spacing Δx, and let the ith (Eulerian) grid cell extend from $x_i = i\Delta x$ to $x_{i+1} = (i + 1)\Delta x$. This Eulerian grid cell is referred to as the arrival cell. The corresponding upstream (Lagrangian) departure cell walls are located at $(x_i)_*$ and $(x_{i+1})_*$, respectively. The width of the departure cell is $(\delta x_i)^n_* = (x_{i+1})^n_* - (x_i)^n_*$. The departure points are usually computed using iterative methods in semi-Lagrangian schemes (see, e.g., Staniforth and Côté 1991) whereas Eulerian schemes, in general, use Euler's method:

$$(x_i)^n_* = x_i - u^n(x_i)\Delta t, \tag{5}$$

where u is the velocity field and Δt the time step.

When using the PCM, PLM (scheme I of van Leer 1977), and PPM, the subgrid-scale reconstruction in cell i is given by

$$\psi_i(\xi) = \overline{\psi}_i, \tag{6}$$

$$\psi_i(\xi) = \overline{\psi}_i + \frac{1}{2}(\overline{\psi}_{i+1} - \overline{\psi}_{i-1})\left(\xi - \frac{1}{2}\right), \tag{7}$$

and

$$\psi_i(\xi) = \psi^L_i + \xi[\Delta\psi_i + \tilde{\psi}_i(1 - \xi)], \tag{8}$$

respectively, where ξ is a normalized coordinate in the ith cell such that $\xi \in [0, 1]$:

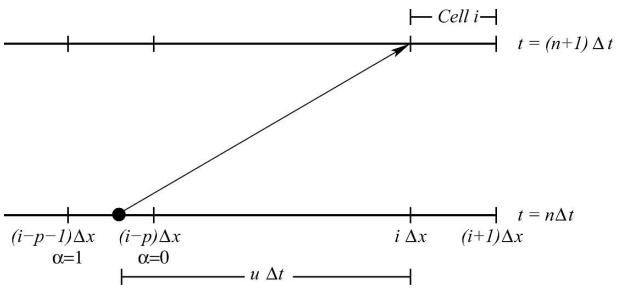

FIG. 1. A space–time representation of the departure and arrival position of the ith left cell wall and the accompanied notation.

$$\xi = \frac{x - x_i}{\Delta x}, \quad x \in [x_i, x_{i+1}], \tag{9}$$

and for the PPM the "slope" and "curvature" of the polynomial are given by

$$\Delta\psi_i = \psi^R_i - \psi^L_i \tag{10}$$

and

$$\tilde{\psi}_i = 6\overline{\psi}_i - 3(\psi^L_i + \psi^R_i), \tag{11}$$

respectively, where $\psi^L_i = \psi_i(0)$ and $\psi^R_i = \psi_i(1)$ are the values of $\psi_i(\xi)$ at the left and right cell walls, respectively, and are computed by interpolation (for details see Colella and Woodward 1984). Performing the subgrid-scale reconstruction from cell averages in all cells defines a global piecewise-continuous function. The reconstructions based on the PLM and PPM can be rendered positive definite and monotonic by applying a posteriori filters (e.g., LR96; Zerroukat et al. 2005). Limiting is a nonlinear process, and hence it is not obvious how to incorporate it into a linear stability analysis. A brief discussion of the implications of using filters on the stability of the schemes is given in section 3d. The subgrid cell reconstruction based on PCM is, of course, shape preserving without the application of filters.

b. Von Neumann stability analysis

Assume a constant wind field $u = u_0 > 0$. Consequently, the exact departure cell is simply the translation of the arrival cell $\Delta t u_0$ units upstream. Let p be the integer value of $u_0\Delta t/\Delta x$, which assures that the departure point corresponding to the arrival point x_i is located in between x_{i-p-1} and x_{i-p} (see Fig. 1). Here p also stands for the integer Courant number. Since the wind field is nondivergent, the prognostic Eq. (3) becomes

$$\overline{\psi}^{n+1}_i = \int_{1-\alpha}^{1} \psi^n_{i-p-1}(\xi)\, d\xi + \int_0^{1-\alpha} \psi^n_{i-p}(\xi)\, d\xi, \tag{12}$$

where $\psi_i(\xi)$ is the subgrid-scale reconstruction polynomial in the cell bounded by x_i and x_{i+1}, and α is the nondimensionalized displacement parameter along the x axis given by

$$\alpha = \frac{u_0 \Delta t}{\Delta x} - p \tag{13}$$

(Fig. 1). When using the PCM for subgrid-scale reconstructions (12) becomes

$$(\overline{\psi}_i)^{n+1}_{\mathrm{PCM}} = \alpha \overline{\psi}_{i-p-1} + (1-\alpha)\overline{\psi}_{i-p}. \tag{14}$$

Assuming that gridpoint values represent cell averages, this formula is formally equivalent to the traditional two-time-level semi-Lagrangian method using linear interpolation or, equivalently, the standard upwind method. When using the PLM and PPM for the subgrid-scale reconstruction, that is, substituting, respectively, (7) and (8) into (12) and evaluating the analytic integrals, (12) can be written as a weighted sum of cell averages

$$(\overline{\psi}_i)^{n+1}_{\mathrm{PLM}} = \frac{1}{4}[-\alpha(1-\alpha)\overline{\psi}_{i-p-2} + \alpha(5-\alpha)\overline{\psi}_{i-p-1} + (4+\alpha)(1-\alpha)\overline{\psi}_{i-p} - \alpha(1-\alpha)\overline{\psi}_{i-p+1}] \quad \text{and} \tag{15}$$

$$(\overline{\psi}_i)^{n+1}_{\mathrm{PPM}} = \frac{1}{12}\{\alpha^2(1-\alpha)\overline{\psi}_{i-p-3} - \alpha(1+7\alpha) \times (1-\alpha)\overline{\psi}_{i-p-2} - 4\alpha(4\alpha^2 - 5\alpha - 2)\overline{\psi}_{i-p-1} - 4(1-\alpha)(4\alpha^2 - 3\alpha - 3)\overline{\psi}_{i-p} + \alpha(1-\alpha) \times (7\alpha - 8)\overline{\psi}_{i-p+1} + \alpha(1-\alpha)^2\overline{\psi}_{i-p+2}\}, \tag{16}$$

respectively. Note that (15) and (16) are not formally equivalent to a traditional semi-Lagrangian scheme using cubic and quintic Lagrange interpolation, respectively, although they require the same stencil. Had the piecewise parabolic method of Laprise and Plante (1995) been applied, (16) would, for constant flows, have been formally equivalent to a traditional semi-Lagrangian scheme based on cubic Lagrange interpolation (Plante 1993).

Following a standard Von Neumann stability analysis (e.g., Haltiner and Williams 1980), assume a solution in the form

$$\overline{\psi}^n_i = \int_{i\Delta x}^{(i+1)\Delta x} \psi^0 \Gamma^n \exp(\hat{\imath} k x)\, dx, \tag{17}$$

where $\hat{\imath}$ is the imaginary unit, ψ^0 the initial amplitude, and $k = 2\pi/L$ is the wavenumber (L is the wavelength). The stability and phase properties of the schemes are assessed by substituting the solution (17) into the respective forecast Eqs. (14), (15), and (16), and subsequently analyzing the complex amplification factor Γ. The stability of a numerical method is governed by the modulus of the complex amplification factor; that is, a particular wave with wavenumber k is stable if $|\Gamma| \leq 1$. Following Bates and McDonald (1982), the dispersion properties of the schemes are assessed by writing the complex amplification factor as

$$\Gamma = |\Gamma| \exp(-\hat{\imath}\omega^* \Delta t), \tag{18}$$

where ω^* is the numerical frequency. Define the relative frequency as $R = \omega^*/\omega$ where ω is the exact frequency given by $ku_0 = (p + \alpha)k\Delta x$. If $R > 1$ the numerical scheme is accelerating and if $R < 1$ the scheme is decelerating compared to the exact solution.

By substituting (17) into (14) and multiplying the resulting complex number with its complex conjugate, the squared modulus of the amplification factor for the cell-integrated scheme based on PCM results is

$$|\Gamma|^2_{\mathrm{PCM}} = 1 - 2\alpha(1-\alpha)c, \tag{19}$$

where $c = 1 - \cos(k\Delta x)$. It is clearly verified that this scheme is unconditionally stable. Similarly, for the scheme based on PLM we get

$$|\Gamma|^2_{\mathrm{PLM}} = 1 - \frac{1}{2}c^2\alpha(1-\alpha)[2 - \alpha(1-\alpha)(2-c)]. \tag{20}$$

When using the PPM for the subgrid cell reconstruction $|\Gamma|^2$ can be written as

$$|\Gamma|^2_{\mathrm{PPM}} = 1 - \frac{1}{9}\alpha^2(1-\alpha)^2c^2[3 - 2(\alpha^2 - \alpha - 5)c - (4\alpha^2 - 4\alpha - 1)c^2 + 2\alpha(1-\alpha)c^3]. \tag{21}$$

For the cell-integrated scheme based on PCM, PLM, and PPM, the numerical frequency ω^* is given in terms of

$$\omega^*_{\mathrm{PCM}}\Delta t = pk\Delta x + \tan^{-1}\left[\frac{\alpha \sin(k\Delta x)}{1 - \alpha c}\right], \tag{22}$$

$$\omega^*_{\mathrm{PLM}}\Delta t = pk\Delta x + \tan^{-1}\left\{\frac{\alpha \sin(k\Delta x)\left[1 + \frac{c}{2}(1-\alpha)\right]}{1 - \alpha c\left[\alpha + \frac{c}{2}(1-\alpha)\right]}\right\}, \tag{23}$$

and

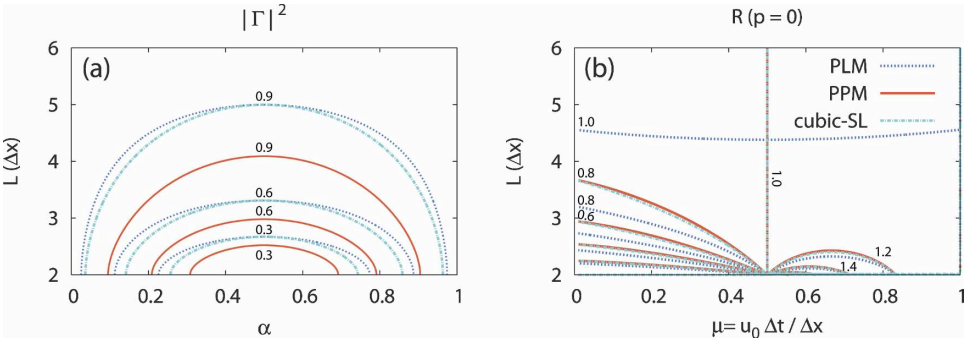

FIG. 2. The stability properties of the one-dimensional finite-volume scheme based on PLM (blue dashed lines) and PPM (red solid lines), respectively, and the traditional semi-Lagrangian scheme using cubic Lagrange interpolation (cyan dashed–dotted line). (a) The squared modulus of the amplification factor as a function of the displacement parameter α and the wavelength L. The contours start at 0.3 and increase monotonically with an increment of 0.3. (b) The relative phase speed of the three schemes. Contours are from 0.2 to 1.4 with an increment of 0.2.

$$\omega^*_{\mathrm{PPM}}\Delta t = pk\Delta x - \tan^{-1}\left\{\frac{\alpha\sin(k\Delta x)\left[1+\frac{c}{3}(1-\alpha^2)+\frac{c^2\alpha}{3}(1-\alpha)\right]}{1-c\alpha^2\left[1+\frac{c}{3}(1+c)(1-\alpha)\right]}\right\}, \tag{24}$$

respectively. The squared modulus of the amplification factor and the relative phase speed for the one-dimensional finite-volume scheme based on PLM and PPM is shown in Figs. 2a,b as a function of displacement parameter α and wavelength L. For comparison, $|\Gamma|^2$ and R for the traditional semi-Lagrangian scheme based on cubic Lagrange interpolation is shown as well. The cell-integrated scheme based on PPM is less damping than the traditional semi-Lagrangian scheme and cell-integrated scheme based on PLM, and the damping is much more scale selective; that is, the $2\Delta x$ wave that is often associated with noise and/or ripples is heavily damped while the longer wavelengths are much less diffused. Regarding dispersion properties, the cell-integrated scheme based on PPM and the traditional semi-Lagrangian scheme are very similar. The relative phase speed error for the cell-integrated scheme using PLM is smaller and different in structure compared to the other schemes.

3. Two-dimensional finite-volume schemes

As mentioned in the introduction, two-dimensional finite-volume schemes can be divided into two categories: first, CISL schemes in which the integral over the departure area is approximated explicitly, and second, flux-form Eulerian schemes in which the fluxes through the arrival cell walls are estimated. These two types of schemes are discussed as follows.

a. Cell-integrated semi-Lagrangian schemes

The first step in a semi-Lagrangian scheme is the estimation of the fluid parcel trajectories. Usually iterative methods are applied, such as the midpoint method that, however, does not include the acceleration, or algorithms such as the schemes of Hortal (2002) and Lauritzen et al. (2006a) that do include estimates of the acceleration. Given the trajectories, the departure cell can be defined and the integral over the departure cell can be approximated. The method for upstream integration can be divided into two categories. Fully two-dimensional approaches (Rančić 1992; Machenhauer and Olk 1998; NM02) that require two-dimensional subgrid cell reconstructions, and cascade methods in which the upstream integral is split into two one-dimensional problems (Rančić 1995; NSS02; Zerroukat et al. 2002). See Machenhauer et al. (2007) for an overview.

For the two-dimensional subgrid cell reconstruction, the following notation is used: let Δx and Δy be the equidistant grid spacing in the x- and y-coordinate directions, with the ijth cell vertices located at $(x, y) = (x_i,$

y_j), (x_i, y_{j+1}), (x_{i+1}, y_j), and (x_{i+1}, y_{j+1}), respectively, where $x_i = i\Delta x$ and $y_j = j\Delta y$. As in the one-dimensional case, normalized spatial position variables inside the ijth cell are defined by

$$(\xi, \eta) = \left(\frac{x - x_i}{\Delta x}, \frac{y - y_j}{\Delta y}\right),$$
$$(x, y) \in [x_i, x_{i+1}] \times [y_j, y_{j+1}], \tag{25}$$

such that $\xi, \eta \in [0, 1]$. The quasi-biparabolic subgrid cell reconstruction used in NM02 is based on the directional fitting of two parabolas based on PPM. The slope and curvature of the parabola in the x- and y-coordinate directions are denoted $\Delta^{\xi}\psi_{ij}$ and $\tilde{\psi}_{ij}^{\xi}$, and $\Delta^{\eta}\psi_{ij}$ and $\tilde{\psi}_{ij}^{\eta}$, respectively. Using standard compass point notations the quasi-biparabolic subgrid cell reconstruction can be written as

$$\psi_{ij}(\xi, \eta) = \overline{\psi}_{ij}^{n} + \psi_{ij}^{W} + \xi[\Delta^{\xi}\psi_{ij} + \tilde{\psi}_{ij}^{\xi}(1 - \xi)] + \psi_{ij}^{S} + \eta[\Delta^{\eta}\psi_{ij} + \tilde{\psi}_{ij}^{\eta}(1 - \eta)], \tag{26}$$

where the right and left boundary values of the x-coordinate piecewise parabolic fit have been replaced with east (E) and west (W), respectively (similar for the y-coordinate direction; see Fig. 3). Note that lower- and higher-order versions of the NM02 scheme could easily be constructed by using higher- or lower-order subgrid cell reconstructions in each coordinate direction. Also, this subgrid cell reconstruction does not include the variation along the diagonals but only variation along the coordinate directions. Fully two-dimensional subgrid cell reconstruction, such as applied by Rančić (1992), requires the computation of nine coefficients, making the method computationally expensive. Some of the diagonal variation can be included more economically by only adding two "cross" terms (Jablonowski et al. 2006).

For the stability analysis only constant flows $[(u, v) = (u_0, v_0)]$ are considered, in which case the departure cell approximations are identical for all schemes, that is, the exact departure cell [the departure cell approximations for the respective schemes under general flow conditions are discussed in Machenhauer et al. (2007)]. So the NM02 forecast is simply the integral of the piecewise quasi-biparabolic distribution defined in terms of $\psi_{ij}^{n}(\xi, \eta)$ over the exact departure area. In the cascade scheme of NSS02 the upstream integral is split into two one-dimensional problems where the PPM is applied in each cascade sweep (see below). As for the NM02 scheme any order of subgrid cell reconstruction can be applied in the cascade scheme.

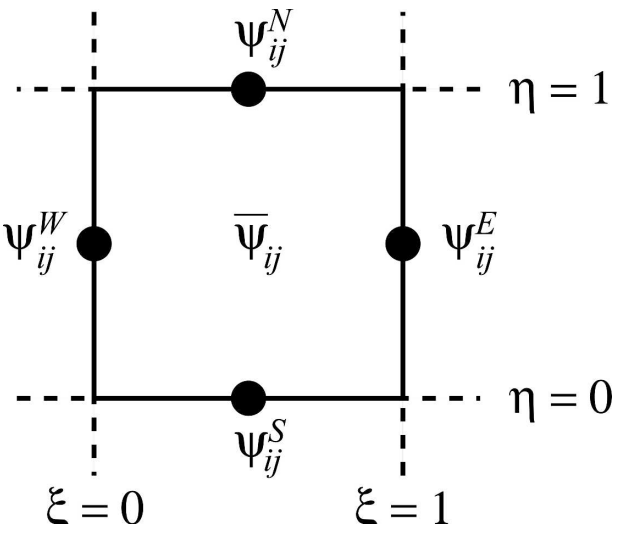

FIG. 3. Graphical illustration of variables used in the quasi-biparabolic subgrid cell reconstruction of the NM02 scheme.

b. Eulerian flux-form scheme

The flux-form scheme of LR96 is based on a Eulerian approach that considers fluxes through the arrival cell walls rather than explicit integration over the departure area as the NM02 and NSS02 schemes do. The LR96 scheme can be written as

$$\overline{\psi}_{ij}^{n+1} = \overline{\psi}_{ij}^{n} + F^{x}\left[\frac{1}{2}(\overline{\psi}^{n} + \mathrm{SL}^{y})\right] + F^{y}\left[\frac{1}{2}(\overline{\psi}^{n} + \mathrm{SL}^{x})\right], \tag{27}$$

where F^x is the difference between the flux through the west and east wall of the arrival cell (similar for F^y). Hence, in terms of the integral operators I, F^x and F^y can be written as

$$F^{x}(\psi) = I^{x}_{(\delta x_i)^{n}_{*}}(\psi) - \overline{\psi}_{ij}^{n} \tag{28}$$

and

$$F^{y}(\psi) = I^{y}_{(\delta y_i)^{n}_{*}}(\psi) - \overline{\psi}_{ij}^{n}, \tag{29}$$

respectively. Here SL^x and SL^y refer to the traditional one-dimensional semi-Lagrangian forecast in the x- and y-coordinate direction, respectively. The "one-dimensional" departure area $(\delta x_{ij})^{n}_{*}$ (letters M, N, O, and P in Fig. 4b) refers to the cell with the west wall located at

$$x = x_i - u_{ij}\Delta t, \tag{30}$$

where u_{ij} is the zonal wind at the center of the west wall of the arrival cell. The south and north walls of the one-dimensional departure cell are at the same lati-

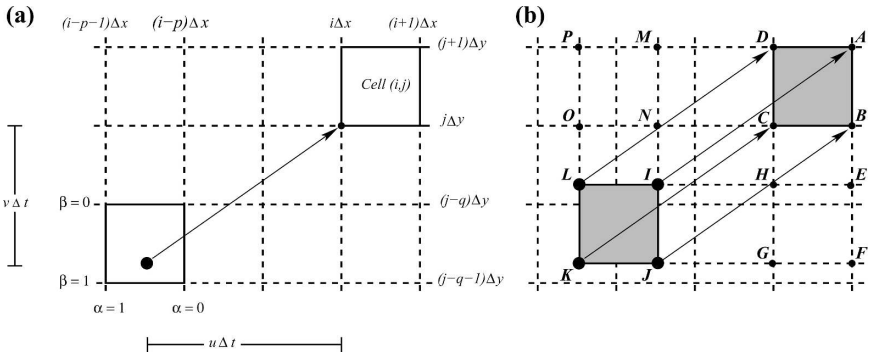

FIG. 4. (a) Same as in Fig. 1 but in two dimensions. The cell bounded by solid lines in the upper right corner is the arrival cell. The departure point corresponding to the southwest vertex of the arrival cell and the arrival point are connected with an arrow. (b) The arrival and departure cell for a constant flow field (shaded areas connected with arrows). The capital letters refer to the points located next to the letter in question and are used to conceptually explain the Eulerian flux-form scheme of LR96.

tudes as the south and north walls of the arrival cell, respectively. Hence the upstream integral is a one-dimensional problem [similar for $(\delta y_{ij})^n_*$ (letters *E*, *F*, *G*, and *H* in Fig. 4b)]. For any scalar *s*, if the flux-form operators F^x and F^y satisfy

$$F(\psi + s) = F(\psi) + F(s) \quad \text{and}$$
$$F(s\psi) = sF(\psi), \tag{31}$$

then (27) can be written as

$$\bar{\psi}_{ij}^{n+1} = \frac{1}{2}[I^x_{(\delta x_{ij})^n_*}(\mathrm{SL}^y) + I^y_{(\delta y_{ij})^n_*}(\mathrm{SL}^x)] + \frac{1}{2}[I^x_{(\delta x_{ij})^n_*} - \mathrm{SL}^x + I^y_{(\delta y_{ij})^n_*} - \mathrm{SL}^y], \tag{32}$$

by utilizing (28) and (29). The operators based on the PCM and unlimited PLM and PPM satisfy (31) (LR96). Following Leonard et al. (1996), (32) can be explained conceptually by assuming a constant flow field, linear interpolations for the SL operators, and PCM for the *I* operators. Under these assumptions the SL and *I* operators are identical. Let $\overline{(ABCD)}$ represent the average of ψ over the cell with vertices *A*, *B*, *C*, and *D*. Using Fig. 4b, terms involved in the forecast are given by

$$I^x_{(\delta x_{ij})^n_*}(\mathrm{SL}^y) = I^y_{(\delta y_{ij})^n_*}(\mathrm{SL}^x) = \overline{(IJKL)}, \tag{33}$$

$$I^x_{(\delta x_{ij})^n_*} = \mathrm{SL}^x = \overline{(MNOP)}, \tag{34}$$

and

$$I^y_{(\delta y_{ij})^n_*} = \mathrm{SL}^y = \overline{(EFGH)}. \tag{35}$$

The terms in the first square brackets on the right-hand side of (32) represent local contributions to the forecast in the sense that the information originates from the exact departure cell (letters *I*, *J*, *K*, and L in Fig. 4b). If one or both of the directional Courant numbers are larger than one then the terms in the second square brackets on the right-hand side of (32) are nonlocal contributions to the forecast because they are evaluated outside the exact departure cell. However, if $\mathrm{SL}^x = I^x_{(\delta x_{ij})^n_*}$ and $\mathrm{SL}^y = I^y_{(\delta y_{ij})^n_*}$, then the nonlocal contributions cancel and (32) becomes $\bar{\psi}_{ij}^{n+1} = \overline{(IJKL)}$, that is, formally equivalent to the upstream CISL scheme. That is, for example, the case when the PCM is used for the *I* operators and linear interpolations in the *SL* operators, and (32) becomes formally equivalent to a traditional semi-Lagrangian scheme using bilinear interpolation (see below). However, if for example the traditional semi-Lagrangian scheme based on linear, quadratic, or cubic interpolation is used for the *SL* operators and PLM or PPM is used for the *I* operators, then SL^z and $I^z_{(\delta z_{ij})^n_*}$, where $z = x, y$, do not cancel. Hence with that particular choice of operators and large Courant numbers there are nonlocal contributions to the forecast that are proportional to the difference between the *SL* and *I* forecasts over the nonlocal areas.

Lin (2004) replaced the SL operators in the LR96 version of the advection scheme with a flux-form operator and subsequently subtracted the divergence; that is,

$$\mathrm{SL}^z = \tilde{I}^z_{(\delta z_{ij})^n_*} - D^z_{(\delta z_{ij})^n_*}\bar{\psi}^n_{ij}, \tag{36}$$

where $z = x, y$, $D^z_{(\delta z_{ij})^n_*}$ is the one-dimensional divergence over $(\delta z_{ij})^n_*$, and $\tilde{I}$ is an integral operator referred to as the

inner integral operator. The integral operator I in (32) is referred to as the *outer* integral operator. Again if the inner and outer operators are the same ($\tilde{I} = I$), the "nonlocal" integral operators in the square brackets in (32) cancel. The divergence terms, however, are nonlocal if Courant numbers are large since the divergence is multiplied with the cell average of ψ over the arrival cell and not the departure cell. In the various implementations of the LR96 advection schemes in models, such as the finite-volume version of the National Center for Atmospheric Research (NCAR) Community Atmosphere Model version 3.0, the choice of inner and outer operators varies with Courant number and location on the spherical domain, and is limited to meridional Courant numbers less than one (S.-J. Lin 2006, personal communication).

c. Von Neumann stability analysis

For the two-dimensional stability analysis assume a constant flow $(u, v) = (u_0, v_0)$, where u_0 and v_0 are positive constants. The x-coordinate displacement parameters α and p are defined in (13), and the y-coordinate displacement parameters β and q are defined similarly (see Fig. 4a). For this purely translational flow the forecast for the different schemes is given in the following subsections.

1) FORECAST FORMULAS

If a constant subgrid cell reconstruction is used in the LR96 scheme then the integral operator is identical to the SL operator using linear interpolation

$$I^x_{(\delta x_{ij})^n_*}(\bar{\psi}) = \mathrm{SL}^x = \alpha\bar{\psi}^n_{i-p-1,j} + (1-\alpha)\bar{\psi}^n_{i-p,j} \tag{37}$$

and

$$I^y_{(\delta y_{ij})^n_*}(\bar{\psi}) = \mathrm{SL}^y = \beta\bar{\psi}^n_{i,j-q-1} + (1-\beta)\bar{\psi}^n_{i,j-q}, \tag{38}$$

and (32) becomes

$$\begin{aligned}\bar{\psi}^{n+1}_{ij} = {} & (1-\alpha)(1-\beta)\bar{\psi}^n_{i-p,j-q} + \alpha(1-\beta)\bar{\psi}^n_{i-p-1,j-q} \\ & + \beta(1-\alpha)\bar{\psi}^n_{i-p,j-q-1} + \alpha\beta\bar{\psi}^n_{i-p-1,j-q-1},\end{aligned} \tag{39}$$

which is formally equivalent to the traditional semi-Lagrangian scheme based on bilinear interpolation. If higher-order operators are applied the explicit equations for $\bar{\psi}^{n+1}_{ij}$ are unfortunately too lengthy to display here.

For a constant flow the cascade scheme of NSS02 can be written as

$$\bar{\psi}^{n+1}_{ij} = I^x_{(\delta x_{ij})^n_*}[I^y_{(\delta y_{ij})^n_*}(\bar{\psi})] = I^y_{(\delta y_{ij})^n_*}[I^x_{(\delta x_{ij})^n_*}(\bar{\psi})], \tag{40}$$

where the PPM is used for the I operators but, of course, any order of integral operator can be applied. For a constant flow $(u, v) = (u_0, v_0)$ and when using I operators without filters/limiters, the order of the "cascade sweeps" can be reversed without influencing the forecast equation; however, that is not the case for general flows and/or when applying limiters (see section 3d). As for the LR96 scheme, the NSS02 scheme reduces to the traditional semi-Lagrangian scheme using bilinear interpolation if the PCM is applied for the I operators. Also, in the Cartesian geometry with uniform grid spacing and for a constant flow $(u, v) = (u_0, v_0)$, the cascade scheme of NSS02 is identical to the scheme of Rančić (1995; reformulated for upstream trajectories).

It is interesting to note that if the inner and outer operators are identical and no filters are applied in the LR96 scheme, it reduces to

$$\begin{aligned}\bar{\psi}^{n+1}_{ij} &= \frac{1}{2}\{I^x_{(\delta x_{ij})^n_*}[I^y_{(\delta y_{ij})^n_*}] + I^y_{(\delta y_{ij})^n_*}[I^x_{(\delta x_{ij})^n_*}]\} && (41)\\ &= I^x_{(\delta x_{ij})^n_*}[I^y_{(\delta y_{ij})^n_*}(\bar{\psi})], && (42)\end{aligned}$$

for a constant flow, since the integral operators under these assumptions commute. In other words, under the assumptions made in the stability analysis, the LR96 scheme with identical inner and outer integral operators is formally identical to the NSS02 cascade scheme. This is, of course, not the case for general flows and/or if limiters are applied. This is discussed briefly in section 3d.

The fully two-dimensional scheme of NM02 can, of course, not be expressed in terms of one-dimensional operators and is given by

$$\begin{aligned}\bar{\psi}^{n+1}_{ij} = {} & \int_{1-\beta}^{1}\int_{1-\alpha}^{1}\psi^n_{i-p-1,j-q-1}(\xi,\eta)\,d\xi\,d\eta \\ & + \int_{1-\beta}^{1}\int_{0}^{1-\alpha}\psi^n_{i-p,j-q-1}(\xi,\eta)\,d\xi\,d\eta \\ & + \int_{0}^{1-\beta}\int_{1-\alpha}^{1}\psi^n_{i-p-1,j-q}(\xi,\eta)\,d\xi\,d\eta \\ & + \int_{0}^{1-\beta}\int_{0}^{1-\alpha}\psi'^n_{i-p,j-q}(\xi,\eta)\,d\xi\,d\eta.\end{aligned} \tag{43}$$

It is easily verified that if the PCM is used [setting $\psi^n_{i-p-1,j-q-1}(\xi, \eta) = \bar{\psi}^n_{i-p-1,j-q-1}$ in (43)] the scheme becomes formally equivalent to the traditional semi-

Lagrangian scheme using bilinear interpolation. The explicit equation for $\overline{\psi}_{ij}^{n+1}$ in the NM02 scheme results from substituting the quasi-biparabolic reconstruction function (26) into (43) and evaluating the analytic integrals. As for the cascade scheme the result is too lengthy to display here, and therefore is omitted.

2) Amplitude and phase analysis

Assume a solution in the form

$$\psi^n(x, y) = \psi^0|\Gamma|^n \exp[\hat{\imath}(k_x x + k_y y)], \qquad (44)$$

where $(k_x, k_y) = (2\pi/L_x, 2\pi/L_y)$ is the wavenumber vector and L_x and L_y are the wavelengths in the two coordinate directions, respectively. As in the one-dimensional analysis, the solution (44) is substituted into the explicit forecast formulas for the respective two-dimensional schemes. Again, if the amplification factor is written as $\Gamma = |\Gamma|\exp(-\hat{\imath}\omega^*\Delta t)$ then the relative frequency is given by $R = \omega^*/\omega$ where the exact frequency is

$$\omega = (p + \alpha)k_x\Delta x + (q + \beta)k_y\Delta y. \qquad (45)$$

Both $|\Gamma|^2$ and R were computed with Maple software, and the explicit formulas for the schemes based on higher-order subgrid cell reconstructions are too lengthy to display here but are, for selected parameters, shown graphically. Multidimensional advection schemes are, in general, the most challenged when the advection is oblique or skew to the grid lines, which can lead to anisotropic distortion of the transported distribution. One might expect the most distortion when the flow is along grid diagonals or slightly off diagonals to avoid any symmetry. For the schemes analyzed here the diagonal flow is the most challenging with respect to damping (not shown). Hence the analysis is restricted to $u_0 = v_0$, unless elsewhere specified explicitly, and only symmetric modes ($k_x = k_y$) are considered. For u_0 or v_0 approaching zero, the schemes degenerate to the one-dimensional cell-integrated scheme analyzed in section 2. Hence $|\Gamma|$ for off-diagonal flow not aligned with the coordinate axis is in between $|\Gamma|$ for the symmetric flow $\alpha = \beta$ (analyzed here) and $|\Gamma|$ for the one-dimensional schemes.

Figures 5 and 6 show the squared modulus of the amplification factor and relative phase speed for the traditional semi-Lagrangian scheme using bicubic interpolation, LR96 for different combinations of outer and inner operators, the two-dimensional NM02 based on PPM, and the NSS02 scheme using PLM and PPM for the one-dimensional cascade sweeps. The CISL schemes, NM02 and NSS02, based on PPM are less diffusive than the traditional semi-Lagrangian scheme based on bicubic interpolation. Of the two CISL schemes based on PPM, the cascade scheme of NSS02 is less diffusive (Figs. 5a,b) apart from the $2\Delta x$ wave (not shown). Unlike the semi-Lagrangian schemes, the squared modulus of the amplification factor for the LR96 scheme using different inner and outer operators is not symmetric about $\alpha = \frac{1}{2}$, which is consistent with the conceptual interpretation of the LR96 scheme. For small displacement parameters the LR96 schemes are less diffusive than the semi-Lagrangian schemes but more diffusive for large α values. The dispersion properties are worse for the LR96 schemes using PCM for the inner operator and higher-order outer operator compared to the semi-Lagrangian schemes for all values of α. The CISL schemes and the traditional semi-Lagrangian schemes based on PPM have similar dispersion properties (Figs. 5c,d). Overall the best scheme with respect to phase errors is the NSS02 scheme based on PLM or equivalently the LR96 scheme using PLM for both the inner and outer operators.

Consistent with the conceptual interpretation of the LR96 scheme, the squared modulus of the amplification factor is not only a function of α but also the integer value of the Courant number, p, if the inner and outer integral operators differ. As discussed in detail in section 3b there can be nonlocal contributions to the forecast for Courant numbers larger than one. Hence the diffusion properties can worsen as p increases. In Fig. 6 the squared modulus of the amplification factor for the LR96 scheme using different combinations of inner and outer operators is shown as a function of Courant number ranging from 0 to 5 and wavelength $L_x = L_y$. For comparison, $|\Gamma|^2$ for the least diffusive combination of operators, the LR96 scheme using PPM for both the inner and outer operator (or equivalently the NSS02 scheme based on PPM), is also shown. In general the LR96 schemes using PCM for the inner operator and a higher-order outer operator (Figs. 6a,c) become more diffusive as the Courant number increases since the nonlocal contributions to the forecast originate from more distant locations (more precisely from the latitude and longitude at which the arrival cell is located) and, as already mentioned, the magnitude of the nonlocal terms is proportional to the difference between the one-dimensional inner and outer operator updates over the nonlocal areas. So the difference between one-dimensional updates based on PPM and PCM, and PLM and PCM, is large enough to produce significant dependence of $|\Gamma|^2$ on p, and for large Courant numbers the dissipation is significantly greater than the semi-Lagrangian schemes. Since the CISL

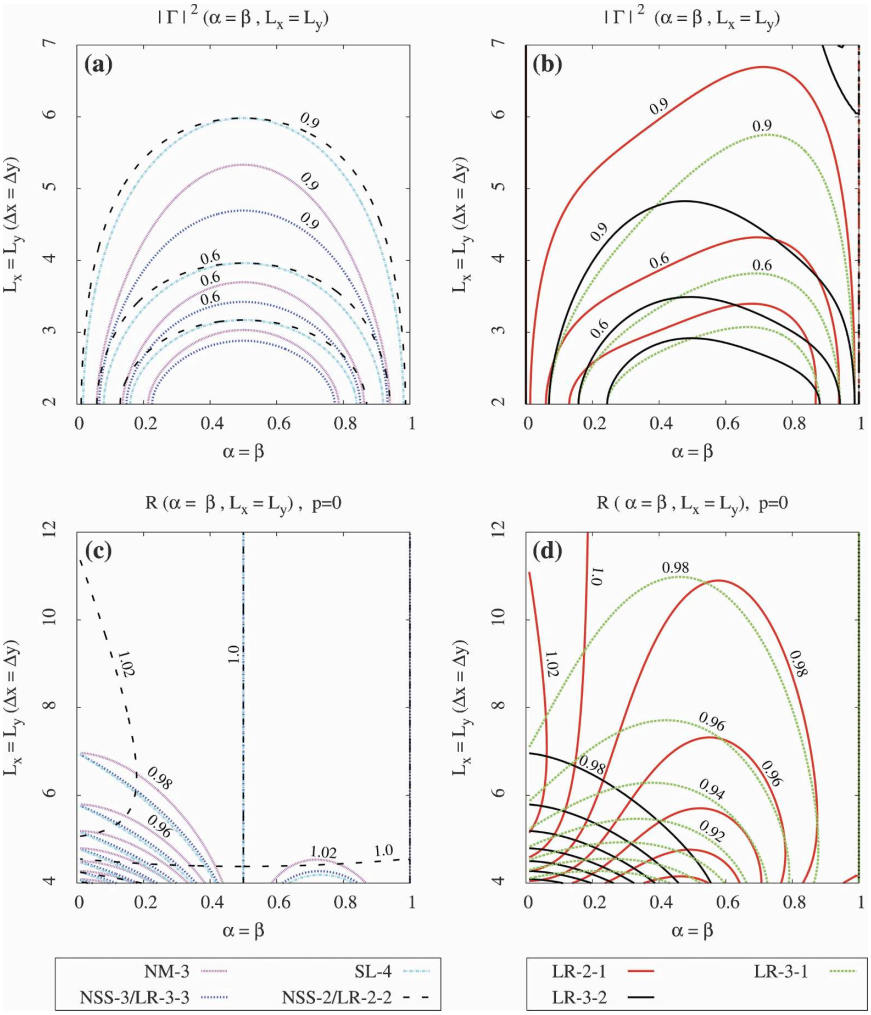

FIG. 5. The stability properties for the traverse waves ($k_x = k_y = 2\pi/L_x = 2\pi/L_y$) as a function of symmetric displacement parameters ($\alpha = \beta$) when using the traditional semi-Lagrangian scheme based on bicubic interpolation (SL-4, cyan dashed–dotted lines), the NM02 scheme (NM-3, pink dotted lines), the cascade scheme of NSS02 using PLM (NSS-2, black dashed lines), and PPM (NSS-3, blue dashed lines), and the LR96 scheme for different combinations of inner and outer operators. For example, LR-3–2 refers to the LR96 scheme using PPM (third order) for the outer operator and PLM (second order) for the inner operator. (a), (b) The squared modulus of the amplification factor as a function of the displacement parameter α and wavelength. (c), (d) Same as in (a) and (b), respectively, but for the relative phase speed. In (b) and (d) $p = 0$ for the LR96 scheme (see also Fig. 6). Note that for a constant flow, $u = u_0$ and $v = v_0$, the LR-3–3 and LR-2–2 schemes are identical to the cascade scheme of NSS02 using PPM and PLM, respectively.

schemes explicitly integrate over the departure cell, $|\Gamma|^2$ is not a function of p for those schemes. The $|\Gamma|^2$ for the LR96 scheme based on the PLM for the inner operator and PPM for the outer operator show little dependence on p, probably because the nonlocal contributions to the forecast, proportional to the difference between the one-dimensional updates over the nonlocal areas using PLM and PPM, are small and less significant. As already mentioned, if the inner and outer operators are identical the dependence on p disappears as the LR96 schemes become formally equivalent to the semi-Lagrangian cascade scheme.

For the LR96 scheme using second-order inner operator (PLM) and third-order outer operator (PPM), $|\Gamma|^2$ can exceed one and is therefore unstable for certain wavelengths and Courant numbers (Fig. 6b). Figure 7 shows the maximum of $|\Gamma|^2$ for this LR96 scheme for different Courant numbers and reveals that the in-

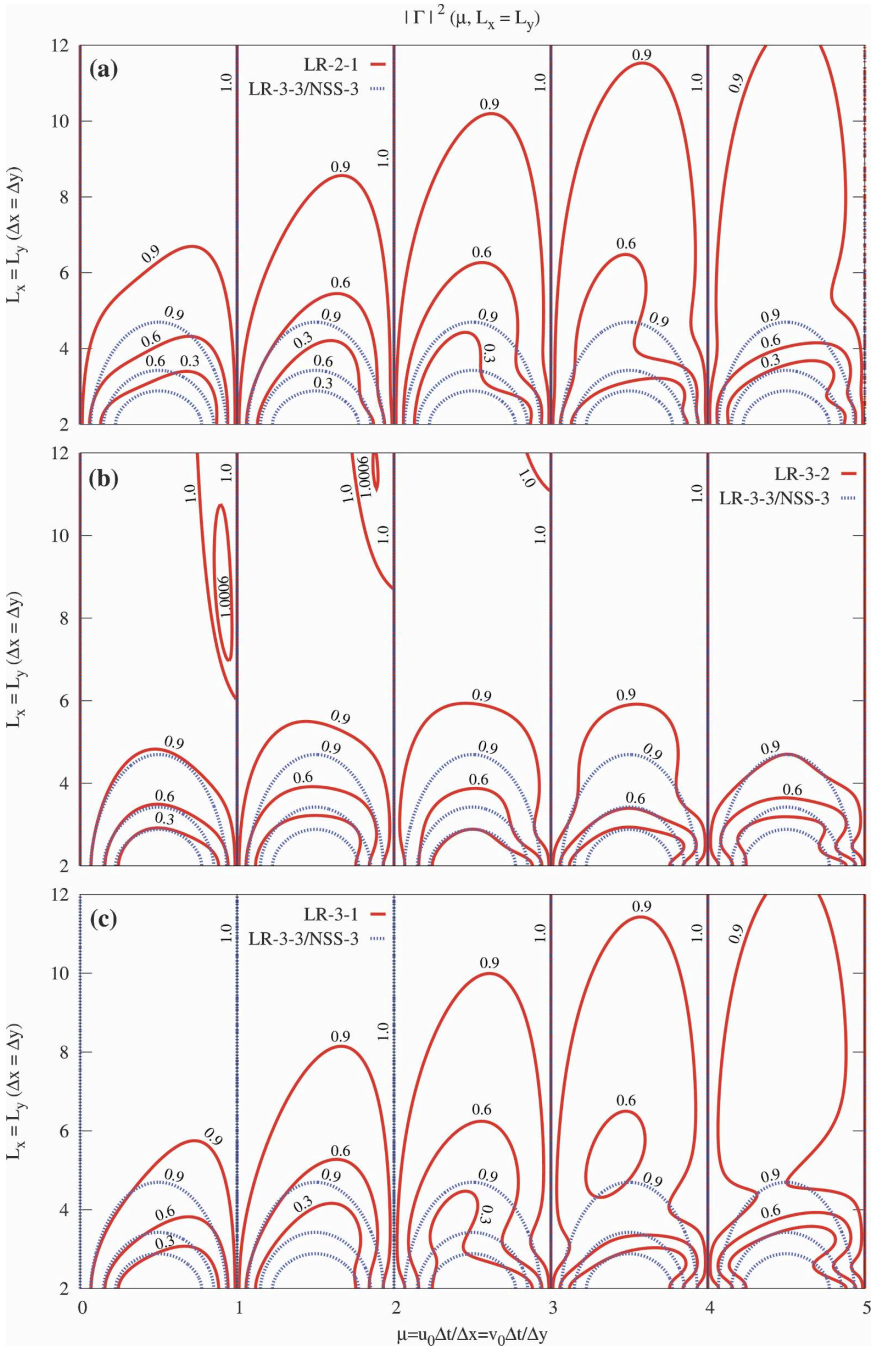

FIG. 6. The figures show the squared modulus of the amplification factor for the LR96 scheme for different combinations of inner and outer operators as a function of symmetric Courant numbers (ranging from 0 to 5) and wavelength. On all figures the dashed blue contours are $|\Gamma|^2$ for the LR96 scheme using PPM for both the inner and outer operators (which renders the scheme identical to the NSS02 scheme based on unlimited PPM under constant flow conditions). Here, $|\Gamma|^2$ for the LR96 scheme with (a) PLM for the outer operator and PCM for the inner operator (LR-2–1), (b) PPM for the outer operator and PLM for the inner operator (LR-3–2), and (c) PPM for the outer operator and PCM for the inner operator (LR-3–1) are shown with contours 0.3, 0.6, 0.9, 1.0, and 1.0006. For fully semi-Lagrangian schemes and the LR96 scheme using identical inner and outer operators the modulus of the amplification factor is not a function of the integer value of the Courant number, p, whereas for the LR96 scheme applying different inner and outer operators $|\Gamma|^2$ is a function of p. A weak instability is present for the LR-3–2 scheme (see also Fig. 7).

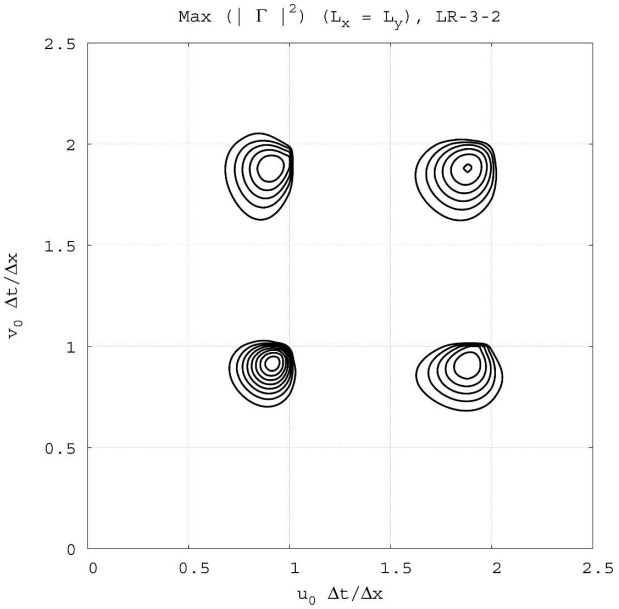

FIG. 7. Maximum of the squared modulus of the amplification factor for symmetric modes ($L_x = L_y$) as a function of x– and y–Courant number for the LR96 scheme using third-order outer operator (PPM) and second-order inner operator (PLM). The contour levels start at 1.0001 and the increment is 0.0001. In most of the domain, maximum ($|\Gamma|^2$) is 1 but for large displacement parameters (α, β) a weak instability is present (maximum of $|\Gamma|^2$ is on the order of 1.0008). See also Fig. 8.

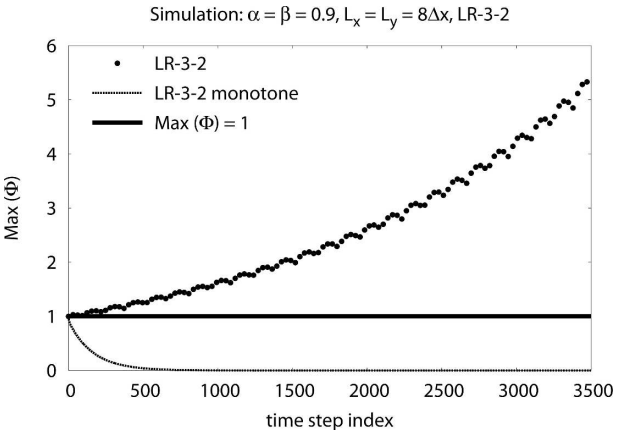

FIG. 8. The maximum of the field as a function of time step index for a simulation with the LR96 scheme using PPM for the outer operator and PLM for the inner operator (LR-3–2) with $\alpha = \beta = 0.9$ and from a $L_x = L_y = 8\Delta x$ initial condition. Filled circles and the dashed line show maximum ($\bar{\psi}$) for the unlimited LR-3–2 scheme and LR-3–2 scheme with a monotonic limiter on the outer operator, respectively. The thick solid line is the neutral damping reference line.

stability is very weak and very scale selective. The squared modulus of the amplification factor is maximum on the order of 1.0008 (for $L_x = L_y \approx 8\Delta x$ and $p = 0$) and, probably, not of any practical importance since the instability is very scale selective and filters are usually applied to the integral operators that may provide significant damping that eliminates the instability. This is indicated by a simulation using the LR96 scheme for advecting the $L_x = L_y = 8\Delta x$ wave with a velocity corresponding to displacement parameters $\alpha = \beta = 0.9$, $p = q = 0$. The maximum of $\bar{\psi}$ over the periodic domain is shown as a function of time step index in Fig. 8. Applying no filters to the integral operators leads to a weakly unstable simulation whereas the application of a monotone filter to the outer operator makes the scheme stable and diffusive. The instability seems only to be of theoretical interest.

d. Brief comments on the general application of the advection schemes

1) THE EFFECT OF LIMITERS/FILTERS

A Von Neumann stability analysis assumes unmodified subgrid cell reconstructions, that is, monotonic and other shape-preserving filters/limiters are not incorporated into the analysis. The use of such filters may result in schemes with very different stability properties compared to the unlimited versions. Schemes with limiters are likely to be more diffusive than their unlimited versions (e.g., Fig. 8). On the contrary the dispersion properties can be positively affected by the use of limiters (e.g., Durran 1999, his Figs. 5.10, 12, 14). It seems reasonable to imagine that the unlimited case provides a baseline from which further dissipation and less dispersion is induced by the limiter/filter. It is noted that the one-dimensional monotonic and positive-definite filters applied in the NM02 and LR96 schemes do not strictly guarantee monotonicity and positive definiteness in two dimensions. In the cascade scheme monotonicity and positive definiteness are guaranteed since they are formulated in terms of two sequential applications of one-dimensional operators for which the filters are strictly shape preserving. It is noted that shape preservation can be enforced in two dimensions in the LR96 scheme such as done by, for example, Skamarock (2006). In the next subsection it is discussed further how spurious negative values can occur in the LR96 and NM02 schemes even though one-dimensional filters are applied, and some of the differences between the LR96 scheme and NSS02 cascade scheme for complex flows are discussed.

2) "SPLITTING ERROR" AND DIRECTIONAL ASYMMETRY

A Von Neumann stability analysis also assumes a constant flow that is nondivergent, nondeformational,

and nonrotational. It is beyond the scope of this analysis to make a comprehensive comparative study of the advection schemes under general flow conditions, but a brief discussion of the differences between the schemes in complex flows is given. All the schemes considered here are based on one-dimensional subgrid cell reconstructions, even the so-called fully two-dimensional CISL scheme of NM02 since the subgrid cell reconstruction is based on the directional fitting of two parabolas, one in each coordinate direction. This can lead to so-called splitting errors and directional biases in the schemes.

First of all, under general flow conditions the cascade scheme is directionally biased, like any tensor-product interpolator, in the sense that the scheme can be applied as

$$\overline{\psi}_{ij}^{n+1} = I_*^{\text{lon}}[I^x_{(\delta x_{ij})_*^n}] \tag{46}$$

or

$$\overline{\psi}_{ij}^{n+1} = I_*^{\text{lat}}[I^y_{(\delta y_{ij})_*^n}], \tag{47}$$

where I_*^{lon} and I_*^{lat} are the one-dimensional integrals along the Lagrangian longitude and latitude (corresponding to an x- and y-isoline transported by the flow), respectively (see NSS02 for details). For the accuracy of the cascade scheme it is important that the Lagrangian longitudes–latitudes are computed with higher-order interpolation (NSS02). For a constant flow, however, $I_*^{\text{lon}} = I^y_{(\delta y_{ij})_*^n}$ and $I_*^{\text{lat}} = I^x_{(\delta x_{ij})_*^n}$, and (46) and (47) are identical to (40). Hence the directional bias does not show in the Von Neumann stability analysis. Under general flow conditions (46) and (47) do not provide identical forecasts. The directional bias can be eliminated with a symmetric cascade scheme by averaging over the two possible versions of (46) and (47),

$$\overline{\psi}_{ij}^{n+1} = \frac{1}{2}\{I_*^{\text{lon}}[I^x_{(\delta x_{ij})_*^n}] + I_*^{\text{lat}}[I^y_{(\delta y_{ij})_*^n}]\}, \tag{48}$$

at the expense of increased computational cost. Four integrals must be evaluated, as in the LR96 scheme, and in addition the Lagrangian longitudes and latitudes must be computed. This extra geometrical work as well as the computation of the trajectories must, however, only be performed once per time step and can be reused for any additional tracers that are advected with the cascade scheme. Alternatively the directional bias can be alleviated in a more cost-effective manner by alternating between (46) and (47).

The averaging of the cross terms is built into the LR96 scheme and hence it is directionally symmetric. For a nondivergent but deformational and rotational flow, the LR96 scheme applying identical inner and outer operators can be written in a form similar to (48):

$$\overline{\psi}_{ij}^{n+1} = \frac{1}{2}\{I^y_{(\delta y_{ij})_*^n}[I^x_{(\delta x_{ij})_*^n}] + I^x_{(\delta x_{ij})_*^n}[I^y_{(\delta y_{ij})_*^n}]\}, \tag{49}$$

but the outer integral operators are applied along the coordinate axis and not along the characteristics of the flow as in the cascade scheme, that is, the LR96 scheme uses fixed-directional splitting while the cascade scheme uses flow-dependent splitting. This can cause a less accurate approximation to the effective departure cell in the LR96 scheme compared to the NSS02 scheme for general flows (Machenhauer et al. 2007). Therefore the splitting errors in the two schemes are not identical. It is noted that the forecast equation for the cascade scheme (47) does not correspond to the directionally biased Eulerian scheme

$$\overline{\psi}_{ij}^{n+1} = \overline{\psi}_{ij}^{n} + F^x + F^y + F^x(F^y), \tag{50}$$

$$= I^x_{(\delta x_{ij})_*^n}[I^y_{(\delta y_{ij})_*^n}] \tag{51}$$

[LR96, their Eq. (2.20)], which has a first-order splitting error. The formal order of the splitting error in the cascade scheme is difficult to assess theoretically (Purser and Leslie 1991) since it requires a nonconstant flow to trigger the error and thus idealized test cases have, so far, been the only way to get an indication of the error. In fact the order of accuracy of the cascade scheme has been estimated numerically in Nair et al. (2003) and indicated to be at least of second order; however, a truncation error analysis is needed to determine the formal order of accuracy [a formal truncation error analysis of the one-dimensional cascade scheme is given in Zerroukat et al. (2006)]. It seems reasonable to assume that the directional bias and splitting errors would show in a strong deformational flow with distributions exhibiting rapid variation, such as the idealized cyclogenesis test case of Doswell (1984) formulated for the sphere in NM02. In this test case the NM02 and NSS02 schemes did not show significant splitting or directional bias errors judging by the standard error measures as compared to other schemes.

By subtracting the divergence from the inner integral operator in (49), thereby effectively converting the inner operator into an advective operator, the LR96 scheme preserves a constant for a nondivergent flow field. The NM02 and NSS02 schemes do not have that property, which is perhaps the most serious deficiency of CISL schemes. This issue is, perhaps, worth more investigation since it is minimally analyzed and discussed in the literature.

Negative values generated from nonnegative initial conditions (nonmonotonic behavior) in the LR96 and NM02 schemes applying a one-dimensional monotonic filter seem to occur when the cross derivatives of the transported distribution exhibit rapid variation (LR96). The filters in the LR96 scheme and the NM02 scheme are applied along the coordinate directions and hence shape-violating variation along the diagonal may still be present even after the application of one-dimensional filters. For the solid body advection of a cosine bell over the Poles with the respective schemes, the negative values are of the same order of magnitude with the two schemes (cf. NM02, their Table 1) and tiny compared to the large-scale distribution. As already mentioned the cascade scheme is strictly shape preserving when filters are applied since it is a sequential scheme.

4. Summary

The recently developed finite-volume schemes for meteorological applications permitting large time steps have been interpreted conceptually and a theoretical Von Neumann stability analysis of these schemes has been performed. The schemes considered have been developed in the meteorological community and are the flux-form Lin and Rood (1996) scheme, the fully two-dimensional cell-integrated scheme of Nair and Machenhauer (2002), and the cascade scheme of Nair et al. (2002). It is noted that the Lin and Rood (1996) scheme is practically identical to the COSMIC scheme of Leonard et al. (1996). The stability analysis does not assume simplified subgrid cell reconstructions but applies the schemes unmodified. Since high-order subgrid cell reconstructions are applied in the finite-volume schemes analyzed here, the explicit forecast formulas and amplification factors are extensive mathematical expressions and have been computed using symbolic mathematical software (Maple). Regarding dissipation, the cell-integrated schemes based on a fully semi-Lagrangian approach [i.e., based on integrating over cells moving with the flow; scheme of Nair and Machenhauer (2002) and Nair et al. (2002)] perform better than the traditional semi-Lagrangian scheme based on bicubic Lagrange interpolation. Of the two cell-integrated schemes, the cascade scheme (Nair et al. 2002) is less damping. The dispersion properties of the higher-order semi-Lagrangian schemes are very similar.

The Lin and Rood (1996) scheme is formulated in terms of a combination of outer flux-form operators and inner advective or flux-form operators. Although the Lin and Rood (1996) scheme is termed semi-Lagrangian, it is based on a Eulerian flux-form approach in which the flux through cell walls is tracked. A conceptual interpretation of the Lin and Rood (1996) scheme is provided that illustrates how the scheme approximates the integral over a cell moving with the flow as is done explicitly in the cell-integrated semi-Lagrangian (CISL) schemes. Here it is shown that if different inner and outer operators are used, there can be nonlocal contributions to the forecast if one or both of the directional Courant numbers are larger than one. Nonlocal refers to the fact that information to the integral over the cell moving with the flow originates from outside the exact departure cell. The magnitude of the nonlocal contributions is proportional to the difference between inner and outer operator updates over the nonlocal areas. Consequently the Lin and Rood (1996) scheme's dissipation properties worsen for increasing Courant numbers for certain choices of inner and outer operators and produces significantly more damping and dispersion errors than the fully semi-Lagrangian schemes. For higher-order inner and outer operators, the nonlocal contributions are small and do not significantly influence the damping for increasing Courant numbers, and the overall stability properties are very similar to the higher-order cell-integrated semi-Lagrangian schemes although a very weak and scale-selective instability can occur. If the inner and outer operators are identical, the Lin and Rood (1996) scheme is formally equivalent to the cascade scheme (for constant flows and unlimited operators only) and the stability properties are, of course, also identical.

This analysis is only restricted to constant flows since the Von Neumann stability analysis is based on such an assumption. Hence the performance of the various schemes under deformational, rotational, and divergent conditions is not part of such an analysis. Also, the application of filters/limiters is, of course, not part of the Von Neumann stability analysis either. All these issues are briefly discussed.

Acknowledgments. The encouragement and careful reviews of early versions of this manuscript by Ramachandran D. Nair and David L. Williamson are gratefully acknowledged. The correspondence with Shian-Jiann Lin has improved this manuscript. Also thanks to Philip Rasch, Mohamed Zerroukat, Chih-Chieh Chen, and two anonymous reviewers for their helpful comments. The author is grateful to NCAR's Advanced Study Program and Climate Modeling Section for providing necessary support for this research.

APPENDIX

Comments on the Lin and Rood (1996) Stability Analysis

It is noted that LR96's Eqs. (A.6), (A.7), and (B.1) in their appendix are missing some terms. The equation

relevant for this paper is Eq. (B.1), that is, the amplification factor for the LR96 scheme using a first-order inner operator and a second-order outer operator. The correct formula using the notation in LR96 is (S.-J. Lin 2006, personal communication)

$$
\begin{aligned}
A = 1 - \frac{1}{2}\Bigg\{ & 1 - e^{-\hat{\imath}Mk} + c_x e^{-\hat{\imath}Mk}(1 - e^{-\hat{\imath}k}) \\
& \times \left[1 + \frac{1}{4} e^{\hat{\imath}k}(1 - c_x)(1 - e^{-2\hat{\imath}k}) \right] \Bigg\} \\
& \times \{1 + e^{-\hat{\imath}Nl}[1 - c_y(1 - e^{-\hat{\imath}l})]\} \\
& - \frac{1}{2}\Bigg\{ 1 - e^{-\hat{\imath}Nl} + c_y e^{-\hat{\imath}Nl}(1 - e^{-\hat{\imath}l}) \\
& \times \left[1 + \frac{1}{4} e^{\hat{\imath}l}(1 - c_y)(1 - e^{-2\hat{\imath}l}) \right] \Bigg\} \\
& \times \{1 + e^{-\hat{\imath}Mk}[1 - c_x(1 - e^{-\hat{\imath}k})]\}. \qquad \text{(A1)}
\end{aligned}
$$

The stability analysis performed in LR96 considers the minimum and maximum of the modulus of the amplification factor of this particular choice of inner and outer operators. In that case min $|A|$ is not a function of the integer translation parameters M and N. Considering the most damped mode, the $2\Delta x = 2\Delta y$ wave, it can easily be shown that $|A|$ reduces to

$$
|A|_{2\Delta} = \sqrt{(1 - 2c_x + 4c_x c_y - 2c_y)^2}. \qquad \text{(A2)}
$$

Obviously $|A|_{2\Delta}$ is not a function of M and N. For other wavelengths, as described in this paper, the modulus of the amplification factor can be a function of the integer value of the Courant number.

REFERENCES

Bates, J. R., and A. McDonald, 1982: Multiply-upstream, semi-Lagrangian advective schemes: Analysis and application to a multi-level primitive equation model. *Mon. Wea. Rev.,* **110,** 1831–1842.

Bott, A., 1989: A positive definite advection scheme obtained by nonlinear renomalization of advective fluxes. *Mon. Wea. Rev.,* **117,** 1006–1015.

Colella, P., and P. R. Woodward, 1984: The piecewise parabolic method (PPM) for gas-dynamical simulations. *J. Comput. Phys.,* **54,** 174–201.

Doswell, C. A., III, 1984: A kinematic analysis of frontogenesis associated with a nondivergent vortex. *J. Atmos. Sci.,* **41,** 1242–1248.

Durran, D. R., 1999: *Numerical Methods for Wave Equations in Geophysical Fluid Dynamics.* Springer-Verlag, 465 pp.

Godunov, S., 1959: A difference scheme for numerical computation of discontinuous solutions of equations in fluid dynamics. *Mat. Sb.,* **47,** 271.

Haltiner, G. J., and R. T. Williams, 1980: *Numerical Prediction and Dynamic Meteorology.* 2d ed. John Wiley & Sons, 477 pp.

Hólm, E. V., 1995: A fully two-dimensional, nonoscillatory advection scheme for momentum and scalar transport equations. *Mon. Wea. Rev.,* **123,** 536–552.

Hortal, M., 2002: The development and testing of a new two-time-level semi-Lagrangian scheme (SETTLS) in the ECMWF forecast model. *Quart. J. Roy. Meteor. Soc.,* **128,** 1671–1687.

Jablonowski, C., M. Herzog, J. E. Penner, R. C. Oehmke, Q. F. Stout, B. van Leer, and K. G. Powell, 2006: Block-structured adaptive grids on the sphere: Advection experiments. *Mon. Wea. Rev.,* **134,** 3691–3713.

Jöckel, P., R. von Kuhlmann, M. G. Lawrence, B. Steil, C. Brenninkmeijer, P. J. Crutzen, P. J. Rasch, and B. Eaton, 2001: On a fundamental problem in implementing flux-form advection schemes for tracer transport in 3-dimensional general circulation and chemistry transport models. *Quart. J. Roy. Meteor. Soc.,* **127,** 1035–1052.

Laprise, J. P. R., and A. Plante, 1995: A class of semi-Lagrangian integrated-mass (SLIM) numerical transport algorithms. *Mon. Wea. Rev.,* **123,** 553–565.

Lauritzen, P. H., E. Kaas, and B. Machenhauer, 2006a: A mass-conservative semi-implicit semi-Lagrangian limited-area shallow-water model on the sphere. *Mon. Wea. Rev.,* **134,** 1205–1221.

Leonard, B. P., A. P. Lock, and M. K. MacVean, 1996: Conservative explicit unrestricted-time-step multidimensional constancy-preserving advection schemes. *Mon. Wea. Rev.,* **124,** 2588–2606.

Lin, S.-J., 2004: A "vertically Lagrangian" finite-volume dynamical core for global models. *Mon. Wea. Rev.,* **132,** 2293–2307.

——, and R. B. Rood, 1996: Multidimensional flux-form semi-Lagrangian transport schemes. *Mon. Wea. Rev.,* **124,** 2046–2070.

Machenhauer, B., and M. Olk, 1998: Design of a semi-implicit cell-integrated semi-Lagrangian model. Max Planck Institute for Meteorology Tech. Rep. 265, Hamburg, Germany, 76–85.

——, E. Kaas, and P. H. Lauritzen, 2007: Finite volume methods in meteorology. *Special Volume on Computational Methods for the Ocean and Atmosphere,* Elsevier, in press.

Nair, R. D., and B. Machenhauer, 2002: The mass-conservative cell-integrated semi-Lagrangian advection scheme on the sphere. *Mon. Wea. Rev.,* **130,** 649–667.

——, J. S. Scroggs, and F. H. M. Semazzi, 2002: Efficient conservative global transport schemes for climate and atmospheric chemistry models. *Mon. Wea. Rev.,* **130,** 2059–2073.

——, ——, and ——, 2003: A forward-trajectory global semi-Lagrangian transport scheme. *J. Comput. Phys.,* **190,** 275–294.

Plante, A., 1993: Transport de substabces par schémas numériques semi-Lagrangiens intégrés par celluls. M.S. thesis, Physics Department, University of Québec at Montréal, 127 pp. [Available from J. P. Laprise, Physics Department, UQAM, P.O. Box 8888, Stn. Downtown, Montréal, QC H3C 3P8, Canada.]

Purser, R. J., and L. M. Leslie, 1991: An efficient interpolation procedure for high-order three-dimensional semi-Lagrangian models. *Mon. Wea. Rev.,* **119,** 2492–2498.

Rančić, M., 1992: Semi-Lagrangian piecewise biparabolic scheme for two-dimensional horizontal advection of a passive scalar. *Mon. Wea. Rev.,* **120,** 1394–1406.

——, 1995: An efficient, conservative, monotonic remapping for semi-Lagrangian transport algorithms. *Mon. Wea. Rev.,* **123,** 1213–1217.

Skamarock, W. C., 2006: Positive-definite and monotonic limiters for unrestricted-time-step transport schemes. *Mon. Wea. Rev.,* **134,** 2241–2250.

Staniforth, A., and J. Côté, 1991: Semi-Lagrangian integration schemes for atmospheric models—A review. *Mon. Wea. Rev.,* **119,** 2206–2223.

van Leer, B., 1977: Towards the ultimate conservative difference scheme. IV: A new approach to numerical convection. *J. Comput. Phys.,* **23,** 276–299.

Zerroukat, M., N. Wood, and A. Staniforth, 2002: SLICE: A semi-Lagrangian inherently conserving and efficient scheme for transport problems. *Quart. J. Roy. Meteor. Soc.,* **128,** 2801–2820.

——, ——, and ——, 2005: A monotonic and positive-definite filter for a semi-Lagrangian inherently conserving and efficient (SLICE) scheme. *Quart. J. Roy. Meteor. Soc.,* **131,** 2923–2936.

——, ——, and ——, 2006: The parabolic spline method (PSM) for conservative transport problems. *Int. J. Numer. Methods Fluids,* **51,** 1297–1318.